



## Research article

# Optimizing restorative procedure and material selection for pulpotomized primary molars: Mechanical characterization by 3D finite element analysis

Jiahui He<sup>a,d</sup>, Jin Sun<sup>a</sup>, Yun Liu<sup>b</sup>, Wei Luo<sup>c</sup>, Ziting Zheng<sup>d</sup>, Wenjuan Yan<sup>d,\*</sup><sup>a</sup> Department of Endodontics, Shenzhen Stomatology Hospital, Shenzhen, PR China<sup>b</sup> Stomatology Health Care Center, Shenzhen Maternity & Child Healthcare Hospital, Shenzhen, PR China<sup>c</sup> Department of Medical Affairs, Shenzhen Stomatology Hospital, Shenzhen, PR China<sup>d</sup> Department of Stomatology, Nanfang Hospital, Southern Medical University, Guangzhou, PR China

## ARTICLE INFO

## Keywords:

Pulpotomy  
3D-finite element analysis  
Primary molar  
Endocrown

## ABSTRACT

**Purpose:** This study aimed to assess the stress distribution in pulpotomized primary molars with different types of restorative materials using 3D-finite element analysis (FEA), and provide valuable insights into the selection and application of restorative materials, with the ultimate goal of reducing the risk of pulpotomy failure and protecting residual dental tissue.

**Methods:** Four 3D models of pulpotomized primary molars with different restorative materials according to the material and its elastic modulus were analysed: resin composite, stainless steel crowns (SSCs), prefabricated zirconia crowns and endocrowns. The food layer was also designed before vertical and bucco-lingual forces were applied to simulate physiological masticatory conditions. The results were obtained by colorimetric graphs of the von Mises stresses (VMS) in the restoration and tooth remnant. The maximum shear stress on the bonding interfaces and pressure stress on the Mineral trioxide aggregate (MTA)-pulp interfaces were recorded.

**Results:** The results of the 3D-FEA showed that all restorative materials generated stresses and strains on the tooth structure after pulpotomy. In the resin composite group, the marginal enamel exhibited the highest stress peaks. In the zirconia crown and SSC groups, there was a concentration of stress at the dentin-restoration margin. The shear stress concentrations were mainly at the adhesive margins, with lower levels around endocrowns compared to other groups. MTA in the resin composite group experienced more VMS than in the other group. The resin composite group also generated relatively higher pressure stress values at the MTA-pulp interface compared to the other groups.

**Significance:** In the model of primary teeth following pulpotomy, the three types of restorations covering the occlusal surface can effectively reduce the stress on pulp capping materials under occlusal loads, thereby potentially decreasing the risk of pulpotomy failure. In addition, the group of endocrowns demonstrated reduced stress at the bonding interface and in the stress concentration zone near the dentist-restoration edge, making them more effective at protecting residual dental tissue.

\* Corresponding author.

E-mail address: [645613053@qq.com](mailto:645613053@qq.com) (W. Yan).<https://doi.org/10.1016/j.heliyon.2024.e35402>

Received 19 July 2023; Received in revised form 26 July 2024; Accepted 29 July 2024

Available online 30 July 2024

2405-8440/© 2024 Published by Elsevier Ltd.

This is an open access article under the CC BY-NC-ND license

[\(http://creativecommons.org/licenses/by-nc-nd/4.0/\)](http://creativecommons.org/licenses/by-nc-nd/4.0/).

## 1. Introduction

With the continuous advancement in biomaterials and the deepening understanding of dental pulp biology, pulpotomy has emerged as an efficacious pulp therapy modality in limited clinical cases for managing dental caries or traumatic pulp exposure, with the aim of preventing further periapical infection and premature loss of primary teeth [1]. This technique involves the complete removal of infected or inflamed coronary pulp and preservation of radicular pulp through biocompatible material sealing, followed by a tight seal at the coronal end. Although the clinical and radiographic success rates of this procedure have been well established, ensuring the quality of restorations is crucial for the long-term effectiveness of pulp treatment [2]. Class of materials to restore primary teeth is represented by resin composites, but the resin composite by direct techniques are less ideal materials in reason of volumetric polymerization shrinkage which may cause residual stresses during the composite cure [3]. Furthermore, primary teeth with extensive lesions or those treated by pulpotomy are susceptible to secondary dental caries, discoloration, and tooth fractures [4,5]. Therefore, they require an occlusal surface coverage restoration that can withstand the chewing load. Currently, various materials, such as stainless steel crowns (SSCs) and zirconia crowns, are widely utilized for the restoration of primary molars following pulpotomy [6].

As early as the 1950s, due to their convenience and cost-effectiveness, SSCs became the preferred choice of dentists for restoring extensively damaged primary molars with long-term success [7,8]. Primary research indicates that the stability and long-term success rate of SSC repair following pulpotomy in primary molars surpass those of direct fillings [5,9]. However, the presence of fatigue cracks and unsatisfactory aesthetics in stainless steel crowns, which are attributed to the properties of metals, has been found to significantly decrease parental satisfaction [10,11]. Prefabricated zirconia crowns for primary teeth, which were introduced in 2010, have gained popularity due to their superior aesthetics and durability resulting from their excellent biofidelity and mechanical properties, including high elastic modulus and bending strength [6,12]. Although prefabricated crowns offer convenience and rapidity, they fail to achieve satisfactory adaptation, occlusal function, and adjacent contact relations. Therefore, a more precise and convenient method for the restoration of primary teeth is a direction for future research.

Computer-aided design/computer-aided manufacturing (CAD/CAM) endocrowns are another aesthetic alternative to prefabricated crowns to restore extensive primary molar lesions [13]. The use of CAD/CAM technology in restorative dental procedures has become increasingly popular in recent years, particularly for permanent teeth [14,15]. The process involves capturing a digital impression of the damaged tooth, designing the restoration on a computer screen, and then milling the final product from a block of restorative material. Endocrowns produced through CAD/CAM technology, which reduces the need for clinical adjustments and minimizes defects during manufacturing, offer advantages such as enhanced aesthetics, improved fit, durability and long-lasting results [16]. The additional benefits of CAD/CAM endocrowns for primary teeth include the capacity to conserve as much natural tooth structure as possible, reduce the necessity for invasive procedures, and uphold the integrity of the tooth [17]. As a result, they have promising

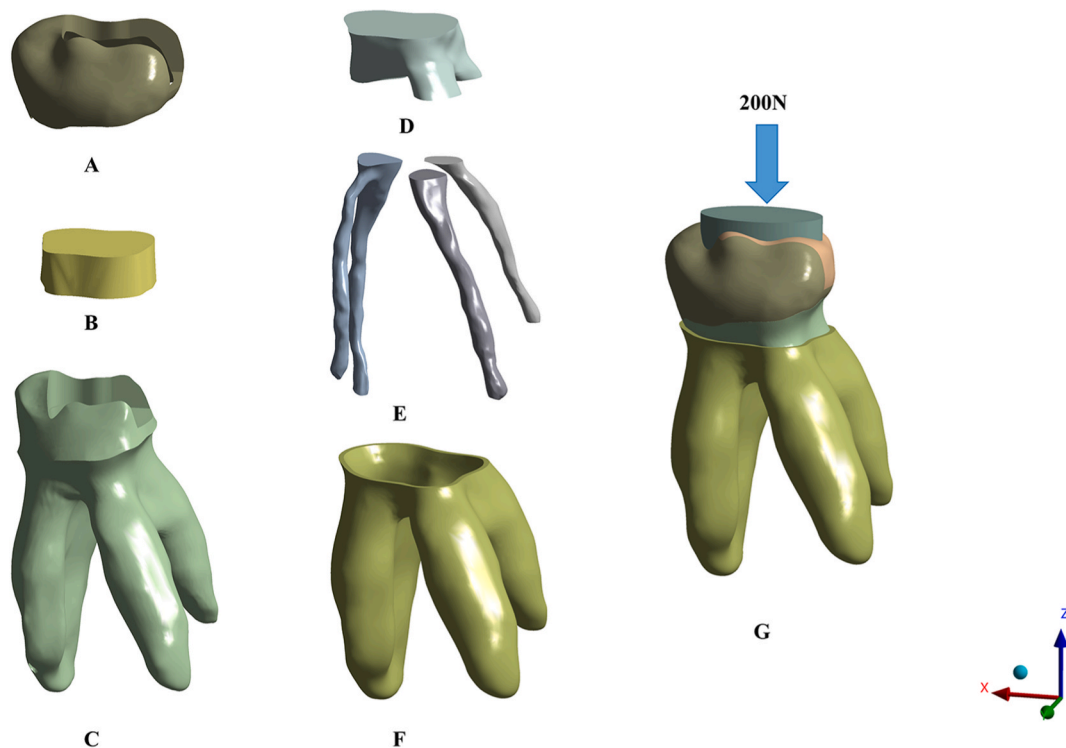


**Fig. 1.** 3D FEA initial model of a molar with Class II cavities that underwent pulpotomy: (A) enamel; (B) glass ionomer cement; (C) dentin; (D) Mineral trioxide aggregate (MTA); (E) pulp; (F) periodontal ligament; (G) static load on the food bolus.

potential in providing full-coverage restoration for primary teeth. Children might also experience less discomfort during the procedure since it can be completed in a single visit without the need for temporaries. However, recent research on pulpotomized primary molars has mostly been conducted through randomized, controlled clinical trials and case reports [18], and further evidence is required to infer the results in an *in vivo* setting.

The application of finite element analysis (FEA) in the field of oral dentistry has been extensive. This analysis effectively simulates various anatomical structures and clinical conditions using mathematical models, providing an efficient approach for optimizing the mechanical behavior of dental structures, prosthetics [19], and implant [20]. FEA is capable of identifying regions with stress concentration, where failures are likely to occur, typically originating from points of higher stress concentrations.

This study aimed to provide valuable insights into the selection and application of restorative materials, by constructing a 3D FEA model of primary molar teeth with pulpotomy, and evaluating the stress distribution of resin composites, SSCs, prefabricated zirconia crowns, and endocrowns in primary molars. The null hypothesis was that there was no difference in the stress distribution in the residual tooth and pulp capping material, regardless of the restorative procedures used.

## 2. Material and method

A 3D CAD model of a healthy primary mandibular first molar (March 2018) was built by means of a microcomputed tomography scan system (Quantum GX; PerkinElmer, Waltham, MA, USA) and CAD software (SolidWorks 2014; Dassault Systèmes, Waltham MA, USA) to generate the shapes of dentin, pulp, enamel, pulp and alveolar bone. All experimental procedures were reviewed and approved by the Local Ethical Committee, Nanfang Hospital, Southern Medical University, Guangzhou, PR China (approval number NFEC-2017-141).

Starting from the 3D CAD model, the trimming tool was utilized to excise a portion of both the enamel and dentin solids, resulting in a slot cavity on the disto-occlusal surface. The facio-lingual dimension of the slot preparation measured 2 mm, while its mesiodistal dimension was 4.5 mm; additionally, its gingival floor lay at a depth of 2 mm below the distal marginal ridge. A solid model was created with a cavity restoration margin angle of  $\alpha = 95^\circ$ . The cavity design featured flat floors and sharp internal line angles. To simulate pulpotomy, the pulp chamber was filled with mineral trioxide aggregate (MTA, Dentsply Tulsa Dental Specialities, OK, USA) to a thickness of 2 mm above the root canal orifice, and the pulp chamber floor was tiled with glass ionomer cement (GIC, Ketac Fil, 3M ESPE, MN, USA). This process resulted in an initial model of a molar with Class II cavities that had undergone pulpotomy (Fig. 1A–F). Four models were modelled for FEA as follows.

**Model 1:** The initial model was restored with resin composite.

**Model 2:** The initial model for SSC was prepared in accordance with the guidelines of 3M ESPE, with a reduction of 1.5 mm on the occlusal surface and 1 mm on the axial walls, which were prepared at an inclination of  $8^\circ$  and finished with feather-edged lines. Subsequently, SSC (3M ESPE, MN, USA) was cemented using GIC (200  $\mu\text{m}$ ) [21].

**Model 3:** The initial model for prefabricated zirconia crowns (Houston, Texas, United States) was prepared based on the primary study [8]. The occlusal surface was reduced by 2 mm, while the axial walls were reduced by 1.5 mm with an inclination of  $8^\circ$  and finish lines of the shoulder (0.5 mm). The zirconia crowns were cemented using resin cement (150  $\mu\text{m}$ ).

**Model 4:** The initial model was prepared for endocrown restoration, featuring a cuspal reduction of 2 mm, a pulp chamber depth of 1 mm, and an  $8^\circ$  inclination angle of the wall. The zirconia endocrowns were cemented using resin cement (150  $\mu\text{m}$ ).

**Model 5:** The control model comprised an intact molar.

The final geometries included the restoration, cement line, enamel, dentin, periodontal ligament, GIC, pulp and alveolar bone (Fig. 1A–G). The interposition of shell elements was utilized to model the cement layer, strategically placed between the intaglio surfaces of the restoration and the bonding surfaces of the residual tooth structure. The simulation of a food bolus [3,22] on the occlusal surface was conducted, incorporating sliding contact between the prosthesis surface and the food (Fig. 1G). In the boundary

**Table 1**

Mechanical properties of materials and structures utilized in this study.

Materials	Modulus of elasticity (GPa)	Poisson's ratio	Modified vol. shrinkage	Linear thermal expansion coefficient
Food [3]	0.010	0.30		
Dentin [22]	18.60	0.31		
Enamel [22]	84.10	0.33		
Cortical bone [22]	13.70	0.30		
Cancellous bone [22]	1.37	0.30		
Pulp [27]	0.0020	0.45		
Glass ionomer cement [21]	10.80	0.30		
MTA [28]	15.70	0.23		
Parodontium [22]	0.069	0.45		
Resin composite [28]	15.80	0.24	0.0010	0.00034
Stainless steel crown [21]	200.00	0.33		
Prefabricated zirconia crown [8]	220.00	0.23		
CAD/CAM zirconia endocrown [8]	220.00	0.23		
Resin cement [29]	7.40	0.35	0.0049	0.0017

condition, the fixation was applied at the base of the bone tissue and was fixed with zero nodal displacements. The assumed properties of all structures were linear-elastic, isotropic, and homogeneously distributed. The mechanical characteristics of the materials and structures, including elasticity moduli and Poisson's ratios, were input into ANSYS software (ANSYS version 14; Swanson Analysis Inc, Canonsburg, USA) (Table 1). In the software environment, the entities were segmented into meshes consisting of nodes and tetrahedral elements. A convergence test with a 10 % mesh control criterion was employed to ascertain the number of elements and nodes necessary for generating four models, as enumerated in Table 2. In this study, a convergence analysis was conducted on grid sensitivity to ensure the reliability of the calculation results, as described in supplementary material.

On account of stress relaxation during the curing process, the shrinkage stresses in composite materials might be lower than those calculated using the elastic model in FEA [23,24]. To consider the simplified approach [23], the modified linear shrinkage of resin materials was adopted in the analyses (Table 1). The resin materials were assigned a linear thermal expansion coefficient to simulate the effects of polymerization shrinkage. Upon a one-degree decrease in temperature, the cement layer underwent contraction, subsequently generating stress at the interface between the substrate and the restoration. To simulate the contact conditions during the closing phase of the masticatory cycle, a static occlusal load of 200 N combined with a bucco-lingual load of 20 N were applied to the surface of the food bolus [25,26].

For all models, the von Mises stresses (VMS) on both restorations and tooth remnants were assessed in megapascals (MPa). The maximum shear stress on bonding interfaces and pressure stress on MTA-pulp interfaces were recorded. This condition is considered a non-failure scenario in the analysis, where all materials were presumed to exhibit elastic behavior throughout the entire deformation process. Slide-type contact elements were employed to model the interface between the tooth surface and food, while no-separation contacts were assumed between the restoration/cement and the cement/tooth interfaces. For all other structural components, the contacts were regarded as ideal. The boundary condition was established at the base of the alveolar bone, where nodal displacements were fixed at zero.

### 3. Results

The colorimetric graphs presented in Figs. 2–6, and Table 3 depicts the distribution of von Mises stresses across the enamel, dentin, pulp, and restorative materials within each model under masticatory loads combined with shrinkage effects. In the resin composite group (Fig. 2A), the marginal enamel adjacent to the resin exhibited higher stress peaks (75.8 MPa), while stresses in the enamel were lower in all of the other groups. The FE models of dentin revealed that VMS were predominantly localized in the upper region of the distal-lingual root base (Fig. 2A–E). The concentration of VMS in the intact molar group was found to be significantly higher than that in all of the other groups. In the zirconia crown and SSC groups, there was a concentration of stress in the upper region of the distal-lingual root located at the dentin-restoration margin. Regarding restoration, VMS were primarily concentrated on the intaglio surface, particularly at the line angle (Fig. 3A–D and Fig. 4A–E). The stress distribution within the restoration was directly proportional to the elastic modulus of the restorative material, meaning that a higher elastic modulus led to increased VMS peak values within the restoration. With regard to internal bonding interface stresses (Fig. 5A–D), it should be noted that shear stress concentrations were primarily concentrated at adhesive margins, with lower levels of shear stress observed around the endocrowns compared to the other groups. The concentrated area of VMS was primarily located at the bottom of MTA, adjacent to the pulp (Fig. 6A–D). In the group with resin composite, the MTA experienced more VMS compared to the other groups (Table 4). With regard to the MTA-pulp interface (Table 3), the resin composite group also generated relatively higher pressure stress values than the other groups.

### 4. Discussion

Traumatic injuries or dental caries can lead to pulp exposure and infection. The aim of pulpotomy treatment is to remove the affected coronal pulp and preserve the viability of the root pulp [1]. The utilization of biocompatible materials in pulp capping, which serves to shield the pulp-dentin complex from external stimuli, can stimulate the formation of dentin bridges by pulp cells and facilitate pulpal healing [30]. A well-executed coronal seal of the final restoration is one of the crucial factors in achieving successful pulpotomy outcomes and ensuring long-term tooth survival [2]. Therefore, the present study was designed to compare the stress distribution in primary molars after pulpotomy that were restored with different operative techniques. The findings indicate that stress concentrations at the residual tooth and pulp capping material can be influenced by different restorative procedures. Thus, the hypothesis was rejected.

Human enamel, possessing the highest elastic modulus among dental tissues and thus being prone to stress concentration, endures repeated masticatory loading during dental function [31,32]. Its integrity directly impacts the success rate of restorations. Compared

**Table 2**  
Number of elements and nodes of five models.

Model	Description	Elements	Nodes
A	Resin composite	399,687	601,376
B	Stainless steel crown	401,078	606,384
C	Prefabricated zirconia crown	394,982	596,558
D	Endocrown	400,571	600,940
E	Intact molar	398,713	592,067

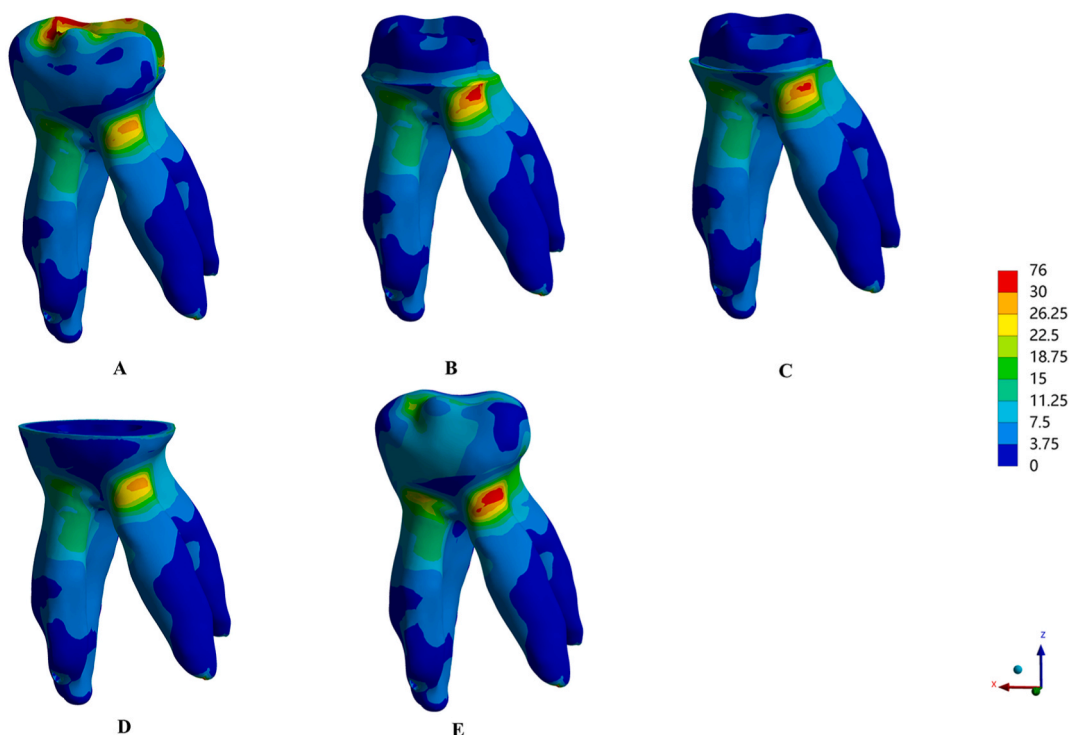


**Fig. 2.** Von Mises stresses (MPa) generated in enamel and dentin according to the restorative material: (A) resin composite; (B) stainless steel crown; (C) zirconia crown; (D) endocrown; (E) intact molar.

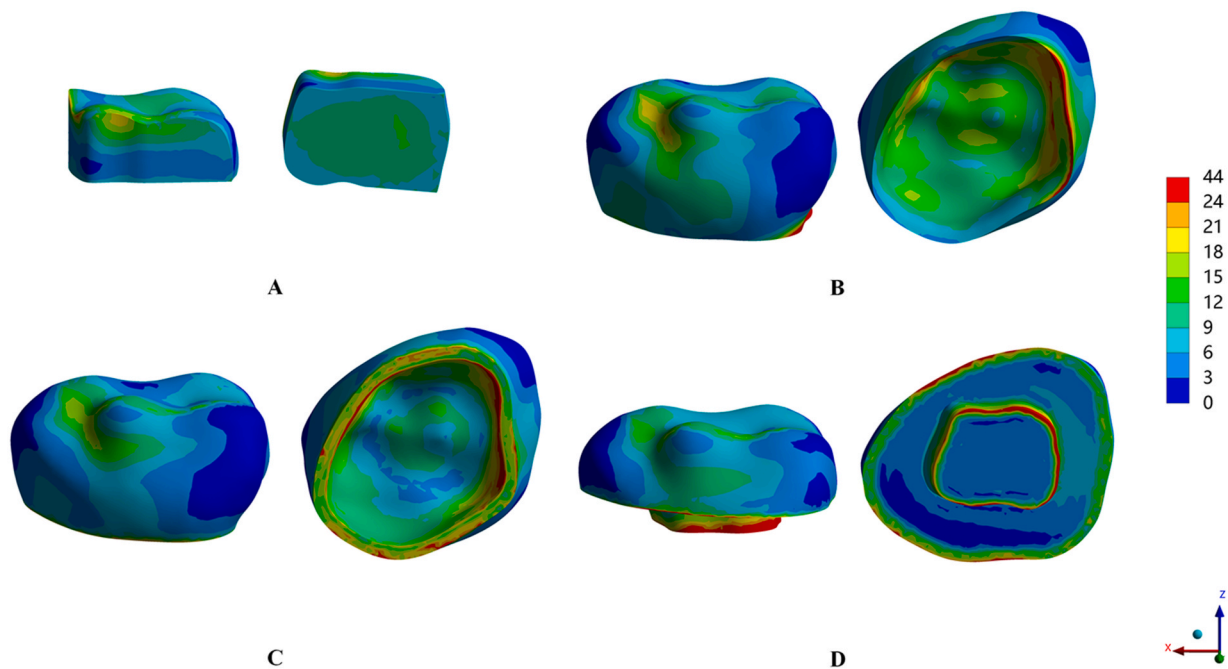


**Fig. 3.** Von Mises stresses (MPa) generated in restoration according to the restorative material: (A) resin composite; (B) stainless steel crown; (C) zirconia crown; (D) endocrown.

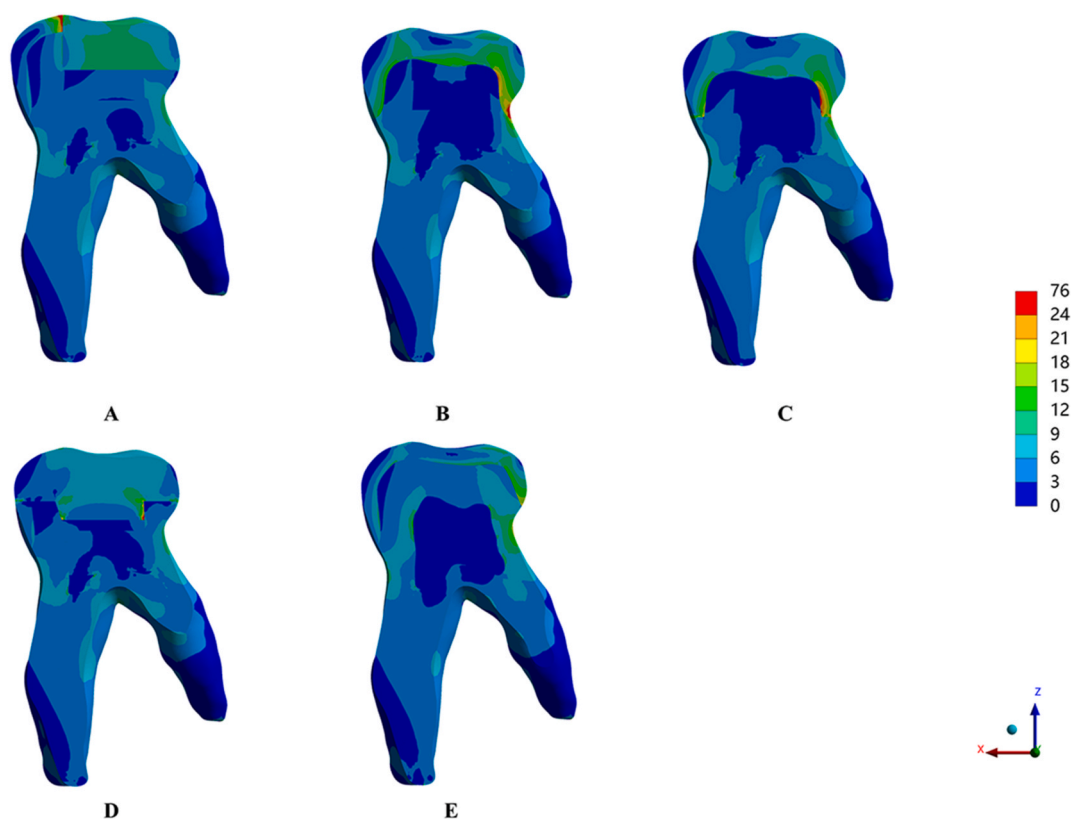


**Fig. 4.** Von Mises stresses (MPa) generated in overall structures on the sagittal plane according to the restorative material: (A) resin composite; (B) stainless steel crown; (C) zirconia crown; (D) endocrown; (E) intact molar.

with intact teeth, SSCs and zirconia crowns, as well as endocrowns, are more effective in reducing equivalent stress on enamel, thus reducing the risk of fracture and better protecting the remaining tooth tissue. The VMS levels in the enamel of primary molars filled with resin composite were significantly higher than those observed in teeth restored by other methods, as well as those present in intact teeth. In the group with resin composite, higher stress peaks were observed in the marginal enamel adjacent to the resin (Fig. 2A), particularly at the mesial margins, which was also the initial area where failure occurred. Due to the distribution of stress and direct effect of masticatory force, there is a possibility that fractures can occur at the enamel margin, resulting in marginal microleakage around the affected restoration [33].

The concentration of VMS is typically observed in the upper region of the distal-lingual root, which can be attributed to the application of a horizontal force (buccal-lingual orientation) during this experiment and the morphology of the mandibular first primary molar. The VMS levels of dentin were found to be lowest in the endocrowns (29.88 MPa) and highest in the SSCs (32.9 MPa). However, it was observed that peak stress values were lower in all restorations compared to intact dentin stress (35.38 MPa), indicating that all rigid prostheses can effectively reinforce tooth structures and significantly reduce the risk of dentin failure under physiological loading conditions. But, in full-crown restorations (including zirconia crowns and SSCs), stress concentration at the upper region of the distal-lingual root located at the dentin-restoration margin can result in dentin fracture and compromise the sealing integrity of margin [34]. Due to the marginal finish line of the prosthesis in the middle of the teeth, the endocrown group remained unaffected.

The restorations in each group exhibited equivalent stress levels far less than the fracture threshold, indicating a limited risk of fracture in restorations (Fig. 3A–D). The stress distribution within endocrowns was relatively uniform and concentrated at the lateral wall of the retainer under identical loading conditions. However, the stresses in full-crown restorations (including zirconia crowns and SSCs) were concentrated specifically at the lateral wall and shoulder of the inner crown (Fig. 3B and C). The stress concentration located at the inner interface of the restoration could pose a potential threat due to its location at the margin interface between the dental tissue and restorations, which can initiate fractures and leakage around the affected restoration [35,36]. Additionally, the stress variations between restorations (Fig. 4A–C) (including resin composite, zirconia crowns and SSCs) and dental tissue were excessive, which could result in stress concentrations at the interfaces, degradation of the cement layer, and an increase in its internal fatigue mechanism [37].

Referring to the internal stress of the bonding interface, it is noteworthy that shear stress concentrations primarily accumulated in the adhesive margin (Fig. 5A–D), and shear stress levels in endocrowns were comparatively lower than those observed in other groups (Table 3). Clinically, the marginal cement between the prosthesis and the abutment is more likely to be directly exposed to the oral environment [38]. Currently, it is believed that the failure of the bonding interface is prone to occur due to excessive stress at the edge.

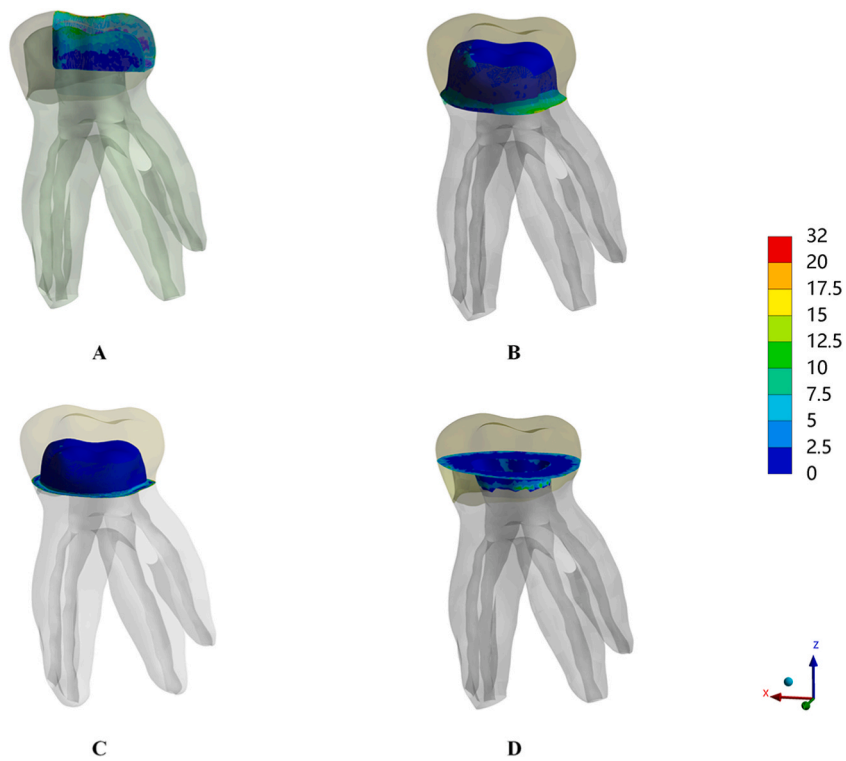


**Fig. 5.** Shear stress (MPa) on bonding interfaces according to the restorative material: (A) resin composite; (B) stainless steel crown; (C) zirconia crown; (D) endocrown.

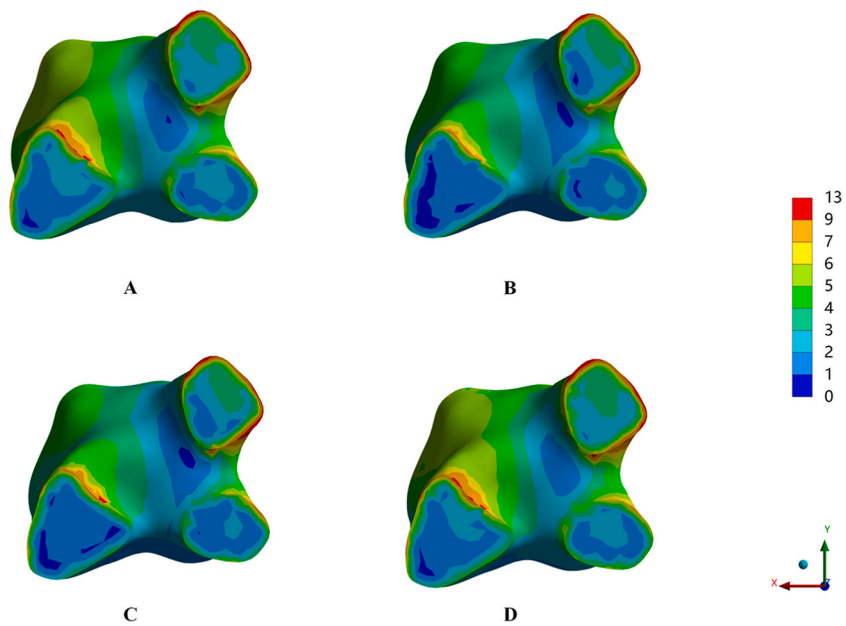


**Fig. 6.** Von Mises stresses (MPa) generated in MTA according to the restorative material: (A) resin composite; (B) stainless steel crown; (C) zirconia crown; (D) endocrown.

When adhesion fails, it can lessen the adhesive effect and initiate detachment of the restoration, thereby leading to secondary caries, pulpitis, and even restoration fracture [39,40]. Our study showed that group of endocrown pruned to reduce stress concentration in the bonding interface and decrease the risk of failure at the edge.

**Table 3**

Von Mises stresses values in restoration, enamel and dentin; shear stress values at the bonding interface under loads (MPa).

	restoration	Enamel	Dentin	bonding interface
Intact teeth		20.05	35.38	
Resin composite	24.78	75.80	29.92	29.33
Stainless steel crown	43.36	13.20	32.90	20.19
Zirconia crown	48.37	14.12	31.86	25.16
Endocrown	42.67	16.61	29.88	16.06

**Table 4**

Von Mises stresses values on MTA; compressive stress values at the MTA-pulp interface according to different restorative techniques.

	MTA	MTA-pulp interface
	VMS ( MPa )	compressive stress ( MPa )
Resin composite	12.95	0.0251
Stainless steel crown	12.21	0.0232
zirconia crown	12.54	0.0225
endocrown	12.47	0.0244

Biocompatibility is a crucial requirement for pulp capping materials, which must possess adequate compressive strength and hardness to withstand occlusal forces [41]. MTA is widely recognized as the gold standard material for pulpotomy procedures, however, studies of its compressive strength have yielded varying results due to factors such as MTA thickness, pulp-penetrating pore size [42], the condensation pressure of MTA [43], and tissue fluid and blood contamination [44,45]. The coronal restorative procedure following pulpotomy not only impacts the marginal fitness and fracture resistance of remaining teeth but also influences the stress distribution within the pulp capping material. The results indicated that the resin composite group directly led to the largest VMS of MTA, and compressive stress on the MTA-pulp interface (Fig. 6A–D, Table 4). According to the reported physiological values of capillary blood pressure (0.0020–0.0047 MPa) [46], although finite element simulation cannot fully replicate the real situation, we believe that the subtle intergroup differences in compressive stress of MTA-pulp interface (0.007–0.0026 MPa) are still significant in Table 4. The compressive stress exerted at the interface between the pulp and MTA directly impacts pulp vitality, with continuous static stress potentially leading to irreversible changes in the neurovascular bundle and an increased risk of pulp necrosis. Therefore, a reduced compressive stress at the MTA-pulp interface is advantageous for safeguarding the integrity of pulp tissue. The three types of restorations covering the occlusal surface can effectively reduce the stress on pulp capping materials under occlusal load, thereby potentially decreasing the risk of pulpotomy failure.

In this study, we developed a model of primary molars and a food bolus fragment to simulate and analyze the impact of closed-cycle chewing on tooth surfaces. However, it is unfeasible to replicate all of the variables present in the oral cavity with computer simulations, such as resistance to cyclic loading, ageing processes, hardness, abrasion and wear. Additionally, this model failed to consider the deficiencies of prefabricated crowns in clinical settings, including suboptimal fit between abutment morphology and restoration, thicker and irregular cement layers [47], high occlusion contact points, and the poor quality of the margin of prefabricated crowns [7], all of which could contribute to decreased fracture resistance. Although VMS, used as the failure criterion in this study, cannot distinguish between compressive and tensile stresses, it provides a simplified method for comprehensively assessing failure risk under multi-axial stress states and is widely applied in engineering practice. Despite the limitations of this study, compared to the resin composite group, the three types of restorations covering the occlusal surface were more effective in reducing the stresses in remaining dental tissue and bonding interfaces, and pulp capping materials. Although the extrapolation of results from in vitro simulations to clinical situations is limited, our findings suggest that endocrowns exhibit superior stress distribution as a restoration option for primary molars following pulpotomy. Specifically, they demonstrated reduced stress at the bonding interface and in the stress concentration zone near the dentin-restoration edge, making them more effective at protecting residual dental tissue. Furthermore, CAD/CAM endocrowns showed potential for future applications due to their superior restoration accuracy and tolerable chair-side operation time [18,19,48]. With the aid of modern digital technology and advancements in dental materials, dentists can achieve optimal results when fabricating primary dental restorations while also ensuring a favourable prognosis for the child.

## 5. Conclusion

Given the constraints of the present study, it may be inferred that restorations covering the occlusal surface demonstrated greater efficacy in reducing stresses within remaining dental tissue, bonding interfaces, and pulp capping materials. CAD/CAM endocrowns with superior restoration accuracy and tolerable chair-side operation time, presented a superior stress distribution, thereby presenting a promising alternative for restoring pulpotomized primary molars.



## Ethics statement

Written informed consent was obtained from all patients for the PUBLICATION of all their data and/or images. The experimental protocol was established in accordance with the ethical guidelines outlined in the Helsinki Declaration and was subsequently approved by the Human Ethics Committee of Nanfang Hospital, Southern Medical University, under approval number NFEC-2017-141.

## Data availability statement

Data will be made available on request.

## Consent for publication

Not applicable.

## CRediT authorship contribution statement

**Jiahui He:** Writing – review & editing, Writing – original draft, Methodology, Investigation, Conceptualization. **Jin Sun:** Methodology, Investigation. **Yun Liu:** Validation, Software, Data curation. **Wei Luo:** Validation, Software. **Ziting Zheng:** Investigation, Formal analysis. **Wenjuan Yan:** Writing – review & editing, Supervision, Conceptualization.

## Declaration of competing interest

The authors declare that they have no known competing financial interests or personal relationships that could have appeared to influence the work reported in this paper.

## Appendix A. Supplementary data

Supplementary data to this article can be found online at <https://doi.org/10.1016/j.heliyon.2024.e35402>.

## References

- [1] N. Tewari, S. Goel, V.P. Mathur, A.C. O'Connell, R.M. Johnson, M. Rahul, F. Sultan, M. Goswami, S. Srivastav, P. Ritwik, Success of medicaments and techniques for pulpotomy of primary teeth: an overview of systematic reviews, *Int. J. Paediatr. Dent.* 32 (2022) 828–842, <https://doi.org/10.1111/ipd.12963>.
- [2] A. Igna, Vital pulp therapy in primary dentition: pulpotomy-A 100-year challenge, *Children* 8 (2021), <https://doi.org/10.3390/children8100841>.
- [3] P. Ausiello, S. Ciaramella, A. Fabianelli, A. Gloria, M. Martorelli, A. Lanzotti, D.C. Watts, Mechanical behavior of bulk direct composite versus block composite and lithium disilicate indirect Class II restorations by CAD-FEM modeling, *Dent. Mater.* 33 (2017) 690–701, <https://doi.org/10.1016/j.dental.2017.03.014>.
- [4] L.A. Chisini, K. Collares, M.G. Cademartori, L.J.C. de Oliveira, M.C.M. Conde, F.F. Demarco, M.B. Correa, Restorations in primary teeth: a systematic review on survival and reasons for failures, *Int. J. Paediatr. Dent.* 28 (2018) 123–139, <https://doi.org/10.1111/ipd.12346>.
- [5] D. Sonmez, L. Duruturk, Success rate of calcium hydroxide pulpotomy in primary molars restored with amalgam and stainless steel crowns, *Br. Dent. J.* 208 (2010) E18, <https://doi.org/10.1038/sj.bdj.2010.446>, discussion 408–409.
- [6] S.L. Pei, M.H. Chen, Comparison of periodontal health of primary teeth restored with zirconia and stainless steel crowns: a systemic review and meta-analysis, *J. Formos. Med. Assoc.* 122 (2023) 148–156, <https://doi.org/10.1016/j.jfma.2022.08.015>.
- [7] N.P. Innes, D.J. Evans, D.R. Stirrups, The Hall Technique; a randomized controlled clinical trial of a novel method of managing carious primary molars in general dental practice: acceptability of the technique and outcomes at 23 months, *BMC Oral Health* 7 (2007) 18, <https://doi.org/10.1186/1472-6831-7-18>.
- [8] C.Y. Pan, T.H. Lan, P.H. Liu, W.R. Fu, Comparison of different cervical finish lines of all-ceramic crowns on primary molars in finite element analysis, *Materials* 13 (2020), <https://doi.org/10.3390/ma13051094>.
- [9] M.V. Korolenkova, A.P. Arzumanyan, Effectiveness of fillings and stainless-steel pediatric crowns for primary molars restoration: the results of prospective randomized split mouth study, *Stomatologiia* 98 (2019) 83–86, <https://doi.org/10.17116/stomat20199803183>.
- [10] J.A. Zimmerman, R. F. M.J. Till, J.S. Hodges, Parental attitudes on restorative materials as factors influencing current use in pediatric dentistry, *Pediatr. Dent.* 31 (1) (2009) 63–70.
- [11] A.C. O'Connell, E. Kratunova, R. Leith, Posterior veneered stainless steel crowns: clinical performance after three years, *Pediatr. Dent.* 36 (2014) 254–258.
- [12] S. Kist, B. Stawarczyk, M. Kollmuss, R. Hickel, K.C. Huth, Fracture load and chewing simulation of zirconia and stainless-steel crowns for primary molars, *Eur. J. Oral Sci.* 127 (2019) 369–375, <https://doi.org/10.1111/eos.12645>.
- [13] D. Papalexopoulos, T.K. Samartzis, A. Sarafianou, A thorough analysis of the endocrown restoration: a literature review, *J. Contemp. Dent. Pract.* 22 (2021) 422–426.
- [14] Y. Nakase, S. Yamaguchi, R. Okawa, K. Nakano, H. Kitagawa, S. Imazato, Physical properties and wear behavior of CAD/CAM resin composite blocks containing S-PRG filler for restoring primary molar teeth, *Dent. Mater.* 38 (2022) 158–168, <https://doi.org/10.1016/j.dental.2021.11.001>.
- [15] Y. Nakase, S. Yamaguchi, E.B.B. Jalkh, P.J. Atria, L. Witek, E.A. Bonfante, H. Li, T. Sakai, R. Okawa, K. Nakano, S. Imazato, In vitro analysis of durability of S-PRG filler-containing composite crowns for primary molar restoration, *Dent. Mater.* 39 (2023) 640–647, <https://doi.org/10.1016/j.dental.2023.04.006>.
- [16] E.I. Oguz, T. Bezgin, A.I. Orhan, K. Orhan, Comparative evaluation of adaptation of esthetic prefabricated fiberglass and CAD/CAM crowns for primary teeth: microcomputed tomography analysis, *BioMed Res. Int.* 2021 (2021) 1011661, <https://doi.org/10.1155/2021/1011661>.
- [17] E. Dursun, A. Monnier-Da Costa, C. Moussally, Chairside CAD/CAM composite onlays for the restoration of primary molars, *J. Clin. Pediatr. Dent.* 42 (2018) 349–354, <https://doi.org/10.17796/1053-4625-42.5.5>.
- [18] M.S. Bilgin, A. Erdem, M. Tanriver, CAD/CAM endocrown fabrication from a polymer-infiltrated ceramic network block for primary molar: a case report, *J. Clin. Pediatr. Dent.* 40 (2016) 264–268, <https://doi.org/10.17796/1053-4628-40.4.264>.
- [19] R.A. Al-Dabbagh, Survival and success of endocrowns: a systematic review and meta-analysis, *J. Prosthet. Dent.* 125 (2021) 415 e411–415 e419, <https://doi.org/10.1016/j.prosdent.2020.01.011>.

- [20] P. Ausiello, J.P.M. Tribst, M. Ventre, E. Salvati, A.E. di Lauro, M. Martorelli, A. Lanzotti, D.C. Watts, The role of cortical zone level and prosthetic platform angle in dental implant mechanical response: a 3D finite element analysis, *Dent. Mater.* 37 (2021) 1688–1697, <https://doi.org/10.1016/j.dental.2021.08.022>.
- [21] A.R. Prabhakar, C.M. Yavagal, A. Chakraborty, S. Sugandhan, Finite element stress analysis of stainless steel crowns, *J. Indian Soc. Pedod. Prev. Dent.* 33 (2015) 183–191, <https://doi.org/10.4103/0970-4388.160352>.
- [22] J. He, Z. Zheng, M. Wu, C. Zheng, Y. Zeng, W. Yan, Influence of restorative material and cement on the stress distribution of endocrowns: 3D finite element analysis, *BMC Oral Health* 21 (2021) 495, <https://doi.org/10.1186/s12903-021-01865-w>.
- [23] P. Kowalczyk, Influence of the shape of the layers in photo-cured dental restorations on the shrinkage stress peaks-FEM study, *Dent. Mater.* 25 (2009) e83–e91, <https://doi.org/10.1016/j.dental.2009.07.014>.
- [24] P. Ausiello, S. Ciaramella, A. Di Rienzo, A. Lanzotti, M. Ventre, D.C. Watts, Adhesive class I restorations in sound molar teeth incorporating combined resin-composite and glass ionomer materials: CAD-FE modeling and analysis, *Dent. Mater.* 35 (2019) 1514–1522, <https://doi.org/10.1016/j.dental.2019.07.017>.
- [25] W.R. Proffit, H.W. Fields, Occlusal forces in normal- and long-face children, *J. Dent. Res.* 62 (1983) 571–574, <https://doi.org/10.1177/00220345830620051301>.
- [26] A.N. Natali, E.L. Carniel, P.G. Pavan, Modelling of mandible bone properties in the numerical analysis of oral implant biomechanics, *Comput. Methods Progr. Biomed.* 100 (2010) 158–165, <https://doi.org/10.1016/j.cmpb.2010.03.006>.
- [27] Z. Kirzioglu, D. Ceyhan, F. Sengul, A.C. Altun, Three-dimensional finite element analysis of the composite and compomer onlays in primary molars, *Comput. Methods Biomech. Biomed. Eng.* 22 (2019) 936–941, <https://doi.org/10.1080/10255842.2019.1604951>.
- [28] M. Brito-Junior, R.D. Pereira, C. Verissimo, C.J. Soares, A.L. Faria-e-Silva, C.C. Camilo, M.D. Sousa-Neto, Fracture resistance and stress distribution of simulated immature teeth after apexification with mineral trioxide aggregate, *Int. Endod. J.* 47 (2014) 958–966, <https://doi.org/10.1111/iej.12241>.
- [29] K. Kitzmuller, A. Graf, D. Watts, A. Schedle, Setting kinetics and shrinkage of self-adhesive resin cements depend on cure-mode and temperature, *Dent. Mater.* 27 (2011) 544–551, <https://doi.org/10.1016/j.dental.2011.02.004>.
- [30] A. Nowicka, M. Lipski, M. Parafiniuk, K. Sporniak-Tutak, D. Lichota, A. Kosierkiewicz, W. Kaczmarek, J. Buczkowska-Radlinska, Response of human dental pulp capped with biodentine and mineral trioxide aggregate, *J. Endod.* 39 (2013) 743–747, <https://doi.org/10.1016/j.joen.2013.01.005>.
- [31] N. Rohr, J. Fischer, Tooth surface treatment strategies for adhesive cementation, *J. Adv. Prosthodont* 9 (2017) 85–92, <https://doi.org/10.4047/jap.2017.9.2.85>.
- [32] S. O'Brien, J. Shaw, X. Zhao, P.V. Abbott, P. Munroe, J. Xu, D. Habibi, Z. Xie, Size dependent elastic modulus and mechanical resilience of dental enamel, *J. Biomech.* 47 (2014) 1060–1066, <https://doi.org/10.1016/j.jbiomech.2013.12.030>.
- [33] B. Dejak, A. Mlotkowski, A comparison of mvM stress of inlays, onlays and endocrowns made from various materials and their bonding with molars in a computer simulation of mastication - FEA, *Dent. Mater.* 36 (2020) 854–864, <https://doi.org/10.1016/j.dental.2020.04.007>.
- [34] N. Forberger, T.N. Gohring, Influence of the type of post and core on in vitro marginal continuity, fracture resistance, and fracture mode of lithia disilicate-based all-ceramic crowns, *J. Prosthet. Dent* 100 (2008) 264–273, [https://doi.org/10.1016/S0022-3913\(08\)60205-X](https://doi.org/10.1016/S0022-3913(08)60205-X).
- [35] N. Sen, Y.O. Us, Mechanical and optical properties of monolithic CAD-CAM restorative materials, *J. Prosthet. Dent* 119 (2018) 593–599, <https://doi.org/10.1016/j.prosdent.2017.06.012>.
- [36] Z. Zheng, J. Sun, L. Jiang, Y. Wu, J. He, W. Ruan, W. Yan, Influence of margin design and restorative material on the stress distribution of endocrowns: a 3D finite element analysis, *BMC Oral Health* 22 (2022) 30, <https://doi.org/10.1186/s12903-022-02063-y>.
- [37] I. Krejci, R. Daher, Stress distribution difference between Lava Ultimate full crowns and IPS e.max CAD full crowns on a natural tooth and on tooth-shaped implant abutments, *Odontology* 105 (2017) 254–256, <https://doi.org/10.1007/s10266-016-0276-z>.
- [38] E. Yuksel, A. Zaimoglu, Influence of marginal fit and cement types on microleakage of all-ceramic crown systems, *Braz. Oral Res.* 25 (2011) 261–266, <https://doi.org/10.1590/s1806-83242011000300012>.
- [39] F. Mannocci, K. Bitter, S. Sauro, P. Ferrari, R. Austin, B. Bhuvan, Present status and future directions: the restoration of root filled teeth, *Int. Endod. J.* 55 (Suppl 4) (2022) 1059–1084, <https://doi.org/10.1111/iej.13796>.
- [40] S. Ghodsi, S. Arzani, M. Shekarian, M. Aghamohseni, Cement selection criteria for full coverage restorations: a comprehensive review of literature, *J Clin Exp Dent* 13 (2021) e1154–e1161, <https://doi.org/10.4317/jced.58671>.
- [41] F.B. Basturk, M.H. Nekoofar, M. Gunday, P.M. Dummer, The effect of various mixing and placement techniques on the compressive strength of mineral trioxide aggregate, *J. Endod.* 39 (2013) 111–114, <https://doi.org/10.1016/j.joen.2012.09.007>.
- [42] Z. Ozkurt-Kayahan, B. Turgut, H. Akin, M.B. Kayahan, E. Kazazoglu, A 3D finite element analysis of stress distribution on different thicknesses of mineral trioxide aggregate applied on various sizes of pulp perforation, *Clin. Oral Invest.* 24 (2020) 3477–3483, <https://doi.org/10.1007/s00784-020-03218-3>.
- [43] M.H. Nekoofar, G. Adusei, M.S. Sheykhrezae, S.J. Hayes, S.T. Bryant, P.M. Dummer, The effect of condensation pressure on selected physical properties of mineral trioxide aggregate, *Int. Endod. J.* 40 (2007) 453–461, <https://doi.org/10.1111/j.1365-2591.2007.01236.x>.
- [44] M.S. Sheykhrezae, N. Meraji, F. Ghanbari, M.H. Nekoofar, B. Bolhari, P.M.H. Dummer, Effect of blood contamination on the compressive strength of three calcium silicate-based cements, *Aust. Endod. J.* 44 (2018) 255–259, <https://doi.org/10.1111/aej.12227>.
- [45] D. Subramanyam, M. Vasantharajan, Effect of oral tissue fluids on compressive strength of MTA and biodentine: an in vitro study, *J. Clin. Diagn. Res.* 11 (2017) ZC94–ZC96, <https://doi.org/10.7860/JCDR/2017/24510.9722>.
- [46] R.A. Moga, R. Cosgarea, S.M. Buru, C.G. Chiorean, Finite element analysis of the dental pulp under orthodontic forces, *Am. J. Orthod. Dentofacial Orthop.* 155 (2019) 543–551, <https://doi.org/10.1016/j.ajodo.2018.05.018>.
- [47] P. Stepp, B.R. Morrow, M. Wells, D.A. Tipton, F. Garcia-Godoy, Microleakage of cements in prefabricated zirconia crowns, *Pediatr. Dent.* 40 (2018) 136–139.
- [48] N. Govare, M. Contrepolis, Endocrowns: a systematic review, *J. Prosthet. Dent* 123 (2020) 411–418 e419, <https://doi.org/10.1016/j.prosdent.2019.04.009>.